

**AERODYNAMIC PERFORMANCE OF USM EFA-1 REMOTELY PILOTED
VEHICLE**

by

ZURRIATI MOHD ALI

**Thesis submitted in fulfilment of the
requirements for the degree
of Master of Science**

May 2004

ACKNOWLEDGEMENTS

In the name of Allah, The Compassionate, The Merciful.

I wish to express my special thanks and gratitude to my supervisor, Assoc. Professor Mohd Zulkifly Abdullah for his constructive involvement in this project. I had the guidance and support from him during this entire process of learning.

My gratitude and appreciation is also conveyed to all the academic and technical staff of the School of Mechanical Engineering, Universiti Sains Malaysia for their assistance directly or indirectly throughout the duration of this work.

I would like to acknowledge that during this work, I had the financial support from *Jabatan Perkhidmatan Awam (JPA)* and Univesiti Teknologi MARA (UiTM).

My special thanks to my parents and family for their support and encouragement during this work. Their patience and compassion are much appreciated.

Last but not least, I wish to express my special thanks to all my fellow colleagues and friends for their invaluable ideas throughout this work.

TABLE OF CONTENTS

| | Page |
|--|------|
| ACKNOWLEDGEMENTS | ii |
| TABLE OF CONTENTS | iii |
| LIST OF TABLES | vi |
| LIST OF FIGURES | vii |
| LIST OF PLATES | x |
| LIST OF SYMBOLS | x |
| LIST OF ABBREVIATION | xi |
| ABSTRAK | xii |
| ABSTRACT | xiii |
| | |
| CHAPTER ONE : INTRODUCTION | 1 |
| | |
| 1.1 REMOTELY PILOTED VEHICLE] | 1 |
| 1.2 BACKGROUND OF THE STUDY | 2 |
| 1.3 SCOPE OF STUDY | 3 |
| 1.4 OBJECTIVE OF STUDY | 4 |
| 1.5 USM's eFA-1 REMOTELY PILOTED VEHICLE | 4 |
| 1.6 THESIS ORGANIZATION | 9 |
| | |
| CHAPTER TWO : LITERATURE REVIEW | 10 |
| | |
| 2.1 AIRCRAFT AERODYNAMIC | 10 |
| 2.1.1 Aerodynamic forces on aircraft | 10 |
| 2.1.2 Reynolds Number | 15 |
| 2.1.3 Airflow around the airfoil | 16 |
| 2.1.4 Effect of vortices | 19 |
| 2.2 REMOTELY PILOTED VEHICLE | 21 |
| 2.2.1 History of flight | 21 |
| 2.2.2 History and development of RPV and UAV | 22 |

| | | |
|---|--|-----------|
| 2.2.3 | Research on RPV and UAV | 27 |
| 2.3 | WIND TUNNEL TESTING | 30 |
| 2.4 | RESEARCH ON THE AEROSPACE ENGINEERING: AERODYNAMIC EXPERIMENTAL METHODS | 32 |
| 2.5 | COMPUTATIONAL FLUIDS DYNAMIC | 37 |
| 2.5.1 | Applications of CFD in aerodynamic studies | 37 |
| 2.5.2 | Application of CFD on experiments | 42 |
| CHAPTER THREE : COMPUTATIONAL SETUP | | 44 |
| 3.1 | SIMULATION PROCEDURE | 45 |
| 3.2 | PRE- PROCESSING | 46 |
| 3.2.1 | Geometry set-up and grid generation | 47 |
| 3.3 | NUMERICAL SIMULATION BY THE SOLVER | 52 |
| 3.3.1 | Solver set-up and solution control | 52 |
| 3.4 | POST PROCESSING | 57 |
| CHAPTER FOUR : RESULTS AND DISCUSSION | | 58 |
| 4.1 | GRID SENSITIVITY | 58 |
| 4.4.1 | Convergence | 63 |
| 4.2 | AERODYNAMIC CHARACTERISTICS OF THE RPV | 65 |
| 4.3 | EFFECT OF REYNOLDS NUMBER | 69 |
| 4.4 | FLOW PATTERN AROUND THE RPV | 71 |
| 4.5 | THE PRESSURE DISTRIBUTION AND VELOCITY VECTORS | 75 |
| 4.5.1 | Around the fuselage | 75 |
| 4.5.2 | Around the wing | 82 |
| CHAPTER FIVE : EXPERIMENTAL APPARATUS AND PROCEDURES | | 88 |
| 5.1 | WIND TUNNEL FACILITY | 88 |
| 5.2 | DESCRIPTION OF THE MODEL | 90 |

| | | |
|--|--|-----|
| 5.2.1 | Similitude analysis | 92 |
| 5.2.2 | Wind tunnel interference | 94 |
| 5.3 | TESTING PROCEDURE | 96 |
| CHAPTER SIX : EXPERIMENTAL RESULTS AND COMPARISON WITH NUMERICAL SIMULATION | | 98 |
| 6.1 | AERODYNAMIC CHARACTERISTIC OF RPV | 98 |
| 6.2 | THE EFFECT OF REYNOLDS NUMBER | 105 |
| 6.3 | ERROR ANALYSIS | 108 |
| 6.4 | COMPARISON OF EXPERIMENTAL AND SIMULATION RESULTS | 113 |
| CHAPTER SEVEN : CONCLUSION AND SUGGESTIONS FOR FUTURE WORK | | |
| 7.1 | CONCLUSION | 121 |
| 7.2 | SUGGESTIONS FOR FUTURE WORK | 123 |
| REFERENCES | | 128 |
| APPENDICES | | 129 |
| | APPENDIX 1 THE RPV FABRICATION PROCESS | 129 |
| | APPENDIX 2 THE RPV FABRICATION PROCESS | 130 |
| | APPENDIX 3 RPV SCALED MODEL | 131 |

LIST OF TABLES

| | Page | |
|-----|--|-----|
| 1.1 | Baseline specifications of eFA-1 RPV [Alfissima et.al, 2001] | 6 |
| 1.2 | The specifications of the Wortmann fx 63-137 [Alfissima et.al, 2001] | 7 |
| 2.1 | The data of UAV [www.auvsi.org] | 25 |
| 3.1 | The turbulence kinetic energy, k and turbulent dissipation rate, ε | 55 |
| 3.2 | Properties of air | 55 |
| 3.3 | Under relaxation factors used in the simulation | 56 |
| 3.4 | Discretization used in the simulation | 56 |
| 3.5 | The reference value used in the simulation | 57 |
| 6.1 | Readings for h1 | 109 |
| 6.2 | Standard deviation calculated for the h1 and h2 readings. | 110 |
| 6.3 | Standard deviation for each set of velocity reading | 111 |

LIST OF FIGURES

| | Page | |
|------|---|----|
| 1.1 | Contour of Wortmann fx 63137 | 7 |
| 1.2 | The schematic diagram of eFA-1 RPV | 8 |
| 2.1 | Aerodynamic forces acting on an aircraft [Barnard and Philpott, 1995] | 11 |
| 2.2 | Streamlines around 2D airfoil [Barnard and Philpott, 1995] | 16 |
| 2.3 | Stream surface [Barnard and Philpott, 1995] | 17 |
| 2.4 | Boundary layer separation [Barnard and Philpott, 1995] | 18 |
| 2.5 | Formation of tip vortex [Bertin and Smith, 1998] | 20 |
| 2.6 | Vortex flow effect [Talay, 1975] | 20 |
| 2.7 | The RPV and UAV with different configurations [www.auvsi.org] | 26 |
| 2.8 | The schematic of the low speed wind tunnel [www.hq.nasa.gov] | 30 |
| 2.9 | Trend in aircraft industry [www.aerodyn.org] | 31 |
| 2.10 | Lift coefficient vs. angle of attack | 34 |
| 2.11 | Drag coefficient vs. angle of attack | 34 |
| 2.12 | Comparison of lift and drag coefficient | 40 |
| 3.1 | Steps in CFD analysis | 46 |
| 3.2 | Three dimensional model of RPV | 48 |
| 3.3 | The surface mesh of RPV | 49 |
| 3.4 | The volume mesh of RPV | 50 |
| 3.5 | Mesh distribution across x-y plane | 50 |
| 3.6 | The boundary conditions setup | 52 |
| 4.1 | The lift curve at Re: 1.05×10^5 | 60 |
| 4.2 | The lift curve at Re: 1.26×10^5 | 60 |
| 4.3 | The lift curve at Re: 1.60×10^5 | 60 |
| 4.4 | The drag curve at Re: 1.05×10^5 | 61 |
| 4.5 | The drag curve at Re: 1.26×10^5 | 61 |
| 4.6 | The drag curve at Re: 1.60×10^5 | 61 |
| 4.7 | The lift to drag ratio against aoa (α) at Re: 1.05×10^5 | 62 |
| 4.8 | The lift to drag ratio against aoa (α) at Re: 1.26×10^5 | 62 |
| 4.9 | The lift to drag ratio against aoa (α) at Re: 1.60×10^5 | 63 |
| 4.10 | The convergence for coarse mesh | 64 |
| 4.11 | The convergence for finer mesh | 64 |
| 4.12 | The lift coefficient for different Reynolds Numbers | 66 |

| | | |
|------|---|----|
| 4.13 | The drag coefficient for different Reynolds Numbers | 67 |
| 4.14 | The drag polar for different Reynolds Numbers | 68 |
| 4.15 | The lift to drag ratio against aoa (α) at different Reynolds Numbers | 69 |
| 4.16 | The lift coefficient for different Reynolds Numbers | 70 |
| 4.17 | The drag coefficient for different Reynolds Numbers | 70 |
| 4.18 | Pressure contours around an aircraft | 72 |
| 4.19 | Pressure contours around the fuselage | 72 |
| 4.20 | Pressure contours on wing | 72 |
| 4.21 | The velocity around the body | 73 |
| 4.22 | The velocity vectors around the fuselage | 74 |
| 4.23 | The velocity vectors around fuselage and wing | 74 |
| 4.24 | (a) – (d): (a) Pressure distribution at $\alpha = 0^\circ$, (b) Pressure distribution at $\alpha = 8^\circ$, (c) Pressure distribution at $\alpha = 12^\circ$, (d) Pressure distribution at $\alpha = 14^\circ$. | 78 |
| 4.25 | (a) - (d): (a) Velocity vector at $\alpha = 0^\circ$, (b) Velocity vector at $\alpha = 8^\circ$, (c) Velocity vector at $\alpha = 12^\circ$, (d) Velocity vector at $\alpha = 14^\circ$. | 81 |
| 4.26 | (a) – (d): (a) Pressure distribution at $\alpha = 0^\circ$, (b) Pressure distribution at $\alpha = 8^\circ$, (c) Pressure distribution at $\alpha = 12^\circ$, (d) Pressure distribution at $\alpha = 14^\circ$. | 84 |
| 4.27 | (a) - (d): (a) Velocity vector at $\alpha = 0^\circ$, (b) Velocity vector at $\alpha = 8^\circ$, (c) Velocity vector at $\alpha = 12^\circ$, (d) Velocity vector at $\alpha = 14^\circ$. | 87 |

| | | |
|------|--|-----|
| 5.1 | The open circuit wind tunnel in Universiti Sains Malaysia | 89 |
| 5.2 | Remotely Piloted Vehicle, eFA-1 prototype | 91 |
| 5.3 | The half scaled model | 92 |
| 5.4 | The photographic image of scale model in the test section | 96 |
| 6.1 | Lift curve at $Re = 1.05 \times 10^5$ | 99 |
| 6.2 | Drag curve at $Re = 1.05 \times 10^5$ | 99 |
| 6.3 | Lift curve at $Re = 1.26 \times 10^5$ | 100 |
| 6.4 | Drag curve at $Re = 1.26 \times 10^5$ | 100 |
| 6.5 | Lift curve at $Re = 1.60 \times 10^5$ | 101 |
| 6.6 | Drag curve at $Re = 1.60 \times 10^5$ | 101 |
| 6.7 | Drag polar at $Re = 1.05 \times 10^5$ | 102 |
| 6.8 | Drag polar at $Re = 1.26 \times 10^5$ | 102 |
| 6.9 | Drag polar at $Re = 1.26 \times 10^5$ | 103 |
| 6.10 | Lift to drag ratio against aoa (α) at $Re = 1.05 \times 10^5$ | 104 |
| 6.11 | Lift to drag ratio against aoa (α) at $Re = 1.26 \times 10^5$ | 104 |
| 6.12 | Lift to drag ratio against aoa (α) at $Re = 1.60 \times 10^5$ | 104 |
| 6.13 | Lift curves at different Reynolds Number | 106 |
| 6.14 | Drag curves at different Reynolds Number | 106 |
| 6.15 | Effect of Reynolds Number on lift coefficients | 107 |
| 6.16 | Effect of Reynolds Number on drag coefficient | 107 |
| 6.17 | The lift curve at $Re = 1.05 \times 10^5$ | 114 |
| 6.18 | The lift curve at $Re = 1.26 \times 10^5$ | 115 |
| 6.19 | The lift curve at $Re = 1.60 \times 10^5$ | 115 |
| 6.20 | The drag curve at $Re = 1.05 \times 10^5$ | 116 |
| 6.21 | The drag curve at $Re = 1.26 \times 10^5$ | 117 |
| 6.22 | The drag curve at $Re = 1.60 \times 10^5$ | 117 |
| 6.23 | The drag polar curve at $Re = 1.05 \times 10^5$ | 118 |
| 6.24 | The drag polar curve at $Re = 1.26 \times 10^5$ | 118 |
| 6.25 | The drag polar curve at $Re = 1.60 \times 10^5$ | 118 |
| 6.26 | The L/D against aoa (α) at $Re = 1.05 \times 10^5$ | 119 |
| 6.27 | The L/D against aoa (α) at $Re = 1.26 \times 10^5$ | 119 |
| 6.28 | The L/D against aoa (α) at $Re = 1.60 \times 10^5$ | 120 |

LIST OF PLATES

- 1 CNC Milling
- 2 Wing part
- 3 Lifting surfaces
- 4 Fuselage and lifting surfaces
- 5 Scaled RPV (1:4)
- 6 Half scaled model (1:5)

LIST OF SYMBOLS

- ρ density
- μ dynamic viscosity of air
- κ turbulence kinetic energy
- ε turbulence dissipation rate]
- α angle of attack
- τ_w shear stress
- a speed of sound
- AC aerodynamic center
- AR aspect ratio
- b wing span
- C_μ constant = 0.09
- c.g center of gravity
- C_D drag coefficient
- C_{dmi} minimum drag coefficient
- C_L^n lift coefficient
- C_{lmax} maximum lift coefficient
- C_M moment coefficient
- CP center of pressure
- C_P pressure coefficient

| | |
|-----------|----------------------|
| D | drag force |
| L | lift force |
| L | length |
| M | Mach number |
| Re | Reynolds number |
| S | wing area |
| S_w | Wing Area |
| TI | turbulence intensity |
| V | velocity |
| V_{max} | maximum velocity |
| V_{so} | stalling speed |
| W_E | Weight empty |
| W_F | Fuel Weight |
| X | length |

LIST OF ABBREVIATION

| | | |
|---------|--|---|
| CFD | Computational Fluids Dynamic | 0 |
| CTRM | Composite Technology Research Malaysia | 0 |
| GUI | Graphical User Guide | 0 |
| LES | Large Eddy Simulation | |
| MAV | Micro Aerial Vehicle | |
| MTOW | Maximum Take off Weight | |
| NASTD | Navier Stokes Time Dependent | |
| RNG | Renormalization - Group | |
| RPV | Remotely Piloted Vehicle | |
| RSM | Reynolds Stress Model | |
| UAV –MR | Unmanned Aerial Vehicle, medium range | |
| UAV | Unmanned Aerial Vehicle | |
| UAV-CR | Unmanned Aerial Vehicle, close range | |
| UAV-E | Unmanned Aerial Vehicle, endurance | |
| UAV-SR | Unmanned Aerial Vehicle, short range | |
| VTOL | Vertical Take off Landing | |
| WIG | Wing-In-Ground | |

PRESTASI AERODINAMIK KE ATAS PESAWAT TANPA JURUTERBANG, USM

EFA-1

ABSTRAK

Pesawat tanpa juruterbang merupakan satu bidang yang agak baru di negara kita Malaysia. Kemajuan terhadap pesawat tanpa juruterbang yang dihasilkan oleh syarikat *Composite Technology Research Malaysia* (CTRM) telah menggalakkan banyak penyelidik dan saintis untuk mempelajari tentang kepentingan dan keupayaan pesawat tanpa juruterbang ini. Dalam kajian ini, penyiasatan terhadap prestasi pesawat tanpa juruterbang, eFA-1 dilakukan melalui kaedah pengkomputeran dan eksperimen. Analisis secara berkomputer telah dilakukan terhadap model pesawat tanpa juruterbang secara tiga dimensi dengan menggunakan Dinamik Bendalir Berkomputer melalui kod FLUENT 6.0. Eksperimen terhadap model skala telah dilakukan dengan menggunakan terowong angin litar terbuka. Penyiasatan dijalankan melalui tiga nombor Reynolds yang berbeza iaitu 1.05×10^5 , 1.26×10^5 dan 1.60×10^5 , dengan kenaikan sudut serang. Sifat-sifat aerodinamik seperti pemalar daya angkat dan daya seretan yang didapati daripada hasil eksperimen akan dibandingkan dengan hasil keputusan berkomputer. Keputusan mendapati bahawa pemalar daya angkat dan daya seretan meningkat dengan kenaikan sudut serang. Pemalar daya angkat maksimum bagi pesawat eFA-1 ialah 0.888 dan pemalar daya seretan minimum ialah 0.037. Sudut tegun berlaku pada $\alpha=14^\circ$. Hasil keputusan daripada simulasi menunjukkan keputusan yang memuaskan bila dibandingkan dengan hasil eksperimen tetapi fenomena sudut tegun tidak dapat diramalkan. Ini disebabkan oleh had yang terdapat pada "model gelora". Gambaran aliran bendalir membantu dalam pemahaman terhadap aliran pada pesawat tanpa juruterbang pada sudut serang yang berbeza. Keputusan yang didapati akan menyediakan data-data aerodinamik bagi eFA-1 untuk kegunaan masa hadapan.

AERODYNAMIC PERFORMANCE OF USM EFA-1 REMOTELY PILOTED VEHICLE

ABSTRACT

Remotely Piloted Vehicle (RPV) in our country Malaysia, still in an early stage. The development of unmanned vehicle by Composite Technology Research Malaysia (CTRM), encourage the local researchers and scientist to study the importance and the capability of RPV. The unique design of RPV is a new challenge for the design engineers and aerodynamicists. In present study, the aerodynamic investigations are carried out on a USM eFA-1 RPV using the computational and experimental methods. The computational analysis is made on a three dimensional model of RPV using computational fluids dynamic (CFD) code FLUENT 6.0. The experimental works are carried on a scale model and tested in an open circuit wind tunnel. The investigations have been carried out at three different Reynolds Numbers, i.e., 1.05×10^5 , 1.26×10^5 and 1.60×10^5 , at different angle of attack. The aerodynamic characteristics lift and drag coefficients obtained from the experimental work are compared to the simulation result. The results show that the lift and drag coefficients are increased with the angle of attack. The maximum lift that can be achieved by the eFA-1 is 0.888 and the minimum drag is 0.037. Stall angle occurs at $\alpha=14^\circ$. The simulation result shows the fairly good agreement with the experimental result but at the stall angle it can't predict the stall phenomena. This is due to the limitation of turbulence model used in this study. The flow pattern helps in better understanding for the flow around the RPV with different angle of attack. The results obtained will provide an aerodynamic database of the eFA-1 RPV for the future use.

CHAPTER ONE

INTRODUCTION

1.1 REMOTELY PILOTED VEHICLE

Remotely piloted vehicle (RPV) is a small aircraft which is fully controlled by human. Remotely piloted refers to the command from people who control the movement of the aircraft using a radio control system. RPV or commonly known as Unmanned Aerial Vehicle (UAV) has a direct continuous link to ground control unit. It can be launched either from ground, vehicle or airplane. There are two categories of UAV, lethal and non-lethal. Lethal UAVs are missile, 'smart weapon', anti-radiation and 'fire and forget' missile with an intelligent guidance system. Non-lethal UAVs are mostly deployed for civil and police task, border patrol, traffic controller, weather inspector and some countries use it for agricultural purposes. UAVs are used widely much more in military as a smart target, reconnaissance vehicle and 'spy-in –the- sky'. The armed forces of United States of America have divided the UAVs into four groups, close range (UAV-CR), short range (UAV-SR), medium range (UAV –MR) and endurance (UAV-E) [Gerken, 1991]. Each group has different endurances, ranges and missions. For non-military, the RPVs are used to search and rescue people, aerial inspection of the housing area, fire detection, traffic control, weather sampling, surveillance of borders and coast. From World War 1 till now, the development of the UAV is still in progress. Many countries are now interested in RPV development, exploiting its full potential and have developed their own UAV programs. In Malaysia, the first development of UAV which is the two

seated aircraft manufactured by Composite Technology Research Malaysia (CTRM), is a stepping stone to start research on the aircraft of what is called 'eyes in the sky'.

1.2 BACKGROUND OF THE STUDY

Aerodynamic means the study of fluid flow and the interaction of the atmosphere around the objects. In aviation, aerodynamic is one of the most important fields to consider when designing a new or modifying the existing airplane. The collections of aerodynamic database, for example lift, drag and moments force will help the designers and aeronautical engineers to improve the aerodynamic design and the performance of the airplane. Since the first airplane has been developed, the design and performance of the airplane is getting better. Many years of studies in aerodynamics leads people to find a way and solutions on how to makes airplane or any flying object to get the maximum capability in speed, performance, ability in any maneuvering and prediction of forces and moment.

At present, the design of UAV is one of the most challenging tasks in aerodynamic studies. In UAV design, the placement of the wing, tail and canard is somehow, not the same as in the conventional airplane configuration. There are a lot of UAV designs such as peanut shape (Canadair CL-227 Sentinel), VTOL UAV with counter-rotating blades and variation of shapes in the planform wings and tails. These configurations need a lot of aerodynamic skills and knowledge to ensure that the UAVs can safely take off, loiter and land.

The aerodynamic development and optimization of UAV is carried out in many countries by organizations, research and development centers and universities. The aerodynamic data are collected from the wind tunnel experiments or by CFD simulation.

There are a numbers of CFD software in the market today which will help aerodynamicists and designers working on their fields efficiently. FLUENT, VSAERO, CFX, PORFLOW, FIDAP and AEROSOFT are examples of CFD codes used by researchers for their numerical simulation works. To date, most of the aerodynamic data collected is based on wind tunnel and computational methods.

1.3 SCOPE OF STUDY

The scope of present study mainly concentrates on getting the basic data on aerodynamic characteristics of the eFA-1 RPV model. This was built at the School of Mechanical Engineering, Universiti Sains Malaysia. During steady flight, there are four main forces subjected on the airplane. These subjected forces are lift, weight, drag and thrust. The parameters that are commonly used to describe aerodynamic characteristics of an aircraft are lift coefficient (C_L), drag coefficient (C_D) and moment coefficient (C_M). These parameters are dependant on the Reynolds number, Re and the angle of attack, α .

In order to obtain the required aerodynamic data, testing was carried out on a scaled model of the RPV in an open circuit wind tunnel and this is also

complemented by using computational simulation in CFD. Experimental tests and CFD simulation are done at different Reynolds numbers and different values of the angles of attack. The results provide the aerodynamic database for the RPV.

1.4 OBJECTIVE OF STUDY

The main objective of the present study is to obtain lift and drag coefficients of eFA-1 RPV. Two different methods are used in this study in order to obtain the aerodynamic characteristics which are experimental and numerical simulation methods. The experimental work was done using the open circuit wind tunnel and the simulation was carried out using the CFD code FLUENT 6.0. The CFD simulation results were validated against the wind tunnel testing results. The results provide the aerodynamic data on eFA-1 RPV for future use.

1.5 USM's eFA-1 REMOTELY PILOTED VEHICLE

In the present study, the RPV model followed the prototype model that was designed by Alfissima et.al [2001]. Alfissima et.al described the method of defining basic parameters that can be used as foundation for further work in the process of designing the UAV prototype. This was the first paper regarding the research work on the development of UAV in the Universiti Sains Malaysia.

Alfissima et.al [2001] have designed and fabricated an unmanned aerial vehicle system and developed the aeronautics design capability. In the project, objective was to build an RPV that is able to carry an optical system to a sufficient height to take aerial images. The vehicle was designed to carry a payload of approximately 4 kg at a cruising altitude of about 1000 m above the sea level and typical operating height at 300 to 600 m above ground. The cruising speed was at 100 km/h and flight durations of about 2 to 4 hours. The mission profiles of the UAV was that it has to perform take off, climb to reach a cruising height of about 1000 m above sea level, cruise flight, loitering, descend and landing. For launching, the RPV was designed to takeoff and land conventionally for the recovery purpose.

The baseline specifications of the RPV were based on the database of typical RPV and UAV that are available in the market. Table 1.1 presents the selected baseline configurations of the RPV that has been made.

Table 1.1: Baseline specifications of eFA-1 RPV [Alfissima et.al, 2001]

| Baseline Specifications | Units |
|--------------------------------|----------------------|
| Payload | ≈ 4kgf |
| Maximum take off weight (MTOW) | ≈ 19kgf |
| Weight empty (W_E) | ≈ 12kgf |
| Fuel Weight (W_F) | ≈ 3kgf |
| Wingspan (b) | ≈ 3m |
| Aspect Ratio (AR) | 8 |
| Wing Area (S_W) | 1.125 m ² |
| Stalling Speed (V_{so}) | 13 m/s |
| Maximum Speed (V_{max}) | 42 m/s |

Airfoil used as the wing section was the Wortmann fx 63-137. The airfoil was designed for low-speed small aircraft. The contour and specifications of the Wortmann airfoil are presented in Figure 1.1 and Table 1.2 respectively.

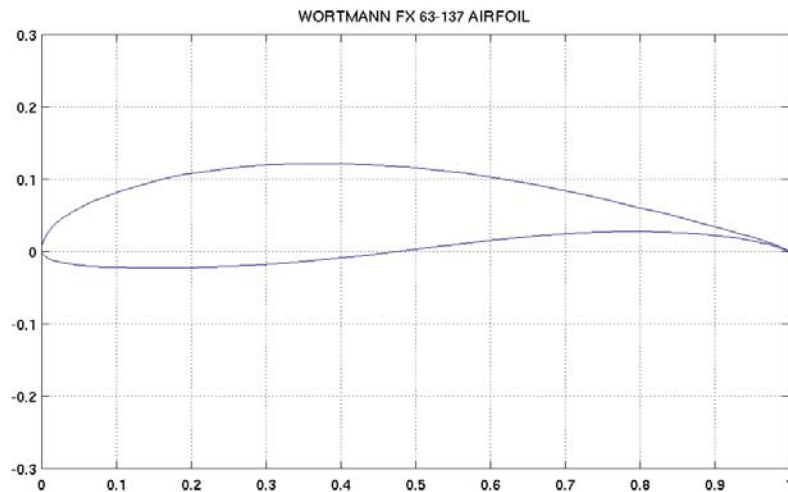


Figure 1.1: Contour of Wortmann fx 63-137

Table 1.2: The specifications of the Wortmann fx 63-137 [Alfissima et.al, 2001]

| | |
|---------------------|-------------------------------------|
| Thickness | 13.68% |
| Maximum camber | 5.83% |
| Leading edge radius | 1.81% |
| Trailing edge angle | 371.842° |
| C_{lmax} | 1.623 (at $Re \sim 3 \times 10^5$) |
| C_{dmin} | 0.014(at $Re \sim 3 \times 10^5$) |
| α_{max} | 13.44°(at $Re \sim 3 \times 10^5$) |

Besides the airfoil selection, the configuration and the planform shape were also considered. The planform of the wing was designed as rectangle because of simplicity and cantilevered. This high wing configuration has been chosen due to its flexibility in operation and also easy to fabricate. At the outer

part of the wing, 3° dihedral angle was added. The incidence angle of the wing was chosen as -2° . This was selected such that the wing should be as efficient as possible during the flight mission with maximum lift over drag ratio.

The AR of the wing is 8. Fiber glass composite will be the major component used in constructing the UAV. However, some parts such as nose area and the area where the landing gear are attached were made of Kevlar to give better durability. Figure 1.2 shows the schematic diagram of eFA-1 RPV.

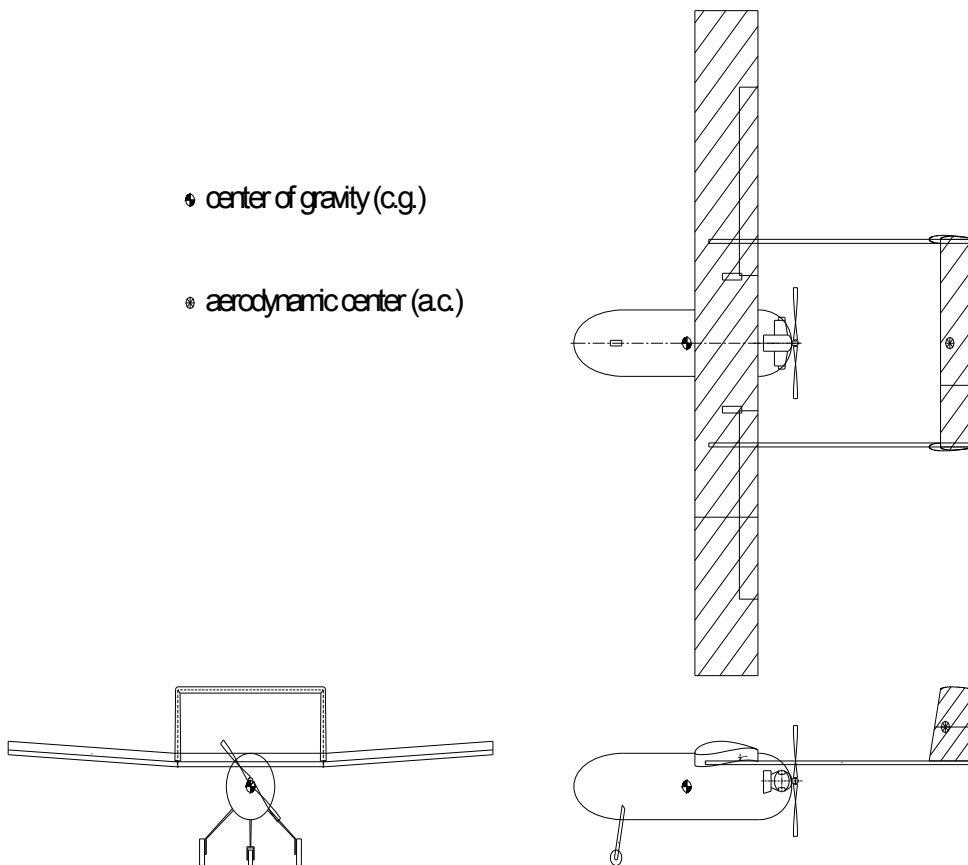


Figure 1.2 : The schematic diagram of eFA-1 RPV

1.6 THESIS ORGANIZATION

Chapter one gives a brief review on the history and background of the research conducted. Research problem is identified in this section, which also defines all objectives to be attained during the research.

Chapter two explores all literature on related works carried out by other researchers. The focus here was on RPV development, aircraft aerodynamics studies and computational study.

Chapter three is based on computational setup and numerical simulation of the scaled RPV of the study.

In chapter four gives detailed analysis of the results obtained from the computational study and the flow pattern behaviour in RPV.

Chapter five describes experimental setup, fabrication of the scaled model, a brief explanation on the wind tunnel testing equipment and testing procedures.

In chapter six, the experimental results have been discussed. Here too the experimental and computational results have been compared and analyzed.

Finally, chapter seven presents the conclusion and possible future works.

CHAPTER TWO

LITERATURE REVIEW

This chapter describes the aircraft aerodynamic, RPV, wind tunnel testing and CFD. The previous research relating to the RPV development and aircraft aerodynamic characteristics are described in detail. Literature survey related to wind tunnel that is used for aircraft testing is also discussed. Finally, a review on CFD and their applications in aerospace researches is presented.

2.1 AIRCRAFT AERODYNAMIC

2.1.1 Aerodynamic forces on aircraft

The forces developed on aircraft are produced by the interaction between the aircraft and the motion of the wind. These forces contribute to the performance of the aircraft whereby it influences the aircraft in speed flight, ascending and descending, take off and landing. During steady constant speed flight, the aircraft is subjected to lift, drag, and weight and thrust forces as shown in Figure 2.1. The aerodynamic coefficients for lift, drag and moment are functions of configuration geometry and attitude.

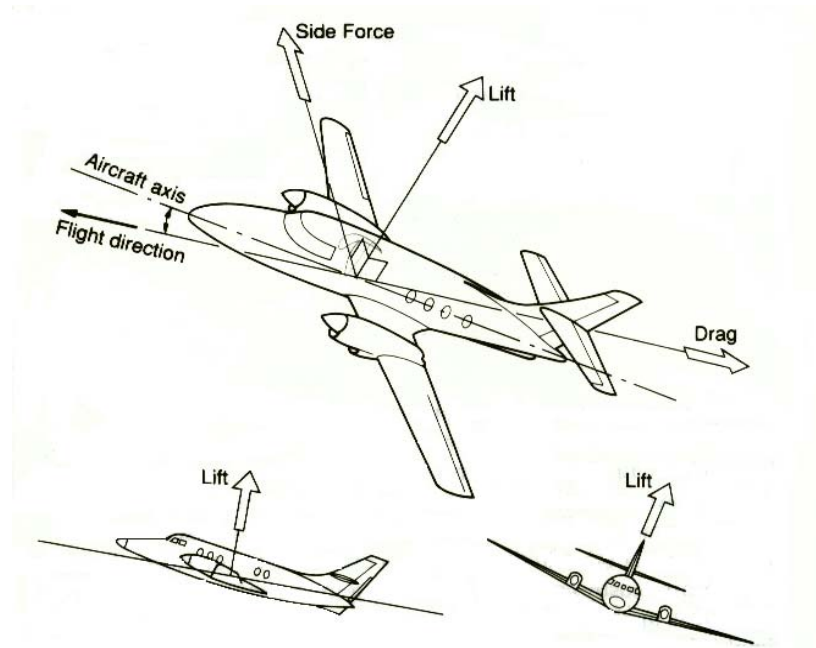


Figure 2.1: Aerodynamic forces acting on an aircraft [Barnard and Philpott, 1995]

The lift is defined as the component of force in the plane of symmetry in a direction perpendicular to the line of flight. For steady level flight; the upward lift force has to be balanced by the aircraft weight. The formula of the lift is:

$$L = \frac{1}{2} \rho V^2 S C_L \quad (2.1)$$

where:

L = lift force

ρ = density

V = velocity

S = reference area

C_L = lift coefficient

For the conventional aircraft, most of the lifts are generated by the wing. When applying the above equation, reference area is referred to the wing planform area which includes the area shadowed by the fuselage [Anderson, 1999]. Horizontal and vertical tail functions control stability and will provide a negative lift or down force. Fuselage and tail also contributes to the lift generation but in a small percentage.

The generation of lift is achieved by producing a greater pressure at the lower surface than upper surface of the body. The difference of the pressure is achieved when the airspeed at the upper surface is higher compared to the lower surface. Inclination of the body relative to the air flow, also contributes to the lift. Lift coefficient measures how efficiently the wing is changing velocity into lift. The higher lift coefficient indicates an efficient airfoil design. The lift coefficient is stated as follows:

$$C_L = \frac{L}{\frac{1}{2}\rho V^2 S} \quad (2.2)$$

Drag in general, is a force that causes a resistance in motion. Drag force is the force developed parallel to the relative wind. Drag force is defined as:

$$D = \frac{1}{2}\rho V^2 S C_D \quad (2.3)$$

where:

D = drag force

ρ = density

V = velocity

S = reference area

C_D = drag coefficient

van Dam [1999] in his review on different methods of drag prediction defines the aerodynamic drag as the sum of tangential or skin friction force and the normal or pressure forces parallel to but in the opposite direction of the vehicle's velocity vector.

Besides the skin friction forces and pressure forces that contribute to the drag of the body, there are other components which are form, viscous, induced and wave drags. Form drag is defined as a dominant component for vehicle with extended region of separated flow. The summation of skin friction and form drag is called viscous or profile drag. In his studies, van Dam also discussed about the induced drag which appear when the vehicle produce a lift. The induced drag is a result of the modification in the vehicle pressure distribution caused by the trailing vortex system that accompanies the production of lift. If one desires to predict a drag through CFD method, van Dam suggested that a critical ingredient for accurate drag prediction are meshes with high resolutions at relevant areas of the flow field and well-developed numerical solvers that do not swamp the flow solution with numerical viscosity. The drag coefficient

measures the efficiency of the wing. Low drag indicates that it is an efficient airfoil.

The drag coefficient is expressed as:

$$C_D = \frac{D}{\frac{1}{2}\rho V^2 S} \quad (2.4)$$

The lift and drag coefficients are related to the lift to drag ratio which is an important term that measures the effectiveness of an aircraft. The lift to drag ratio for a complete aircraft includes not only wing drag but also drags contributed by the rest of the aircraft [Kroes and Rardon, 1993].

$$L/D_{\text{(aircraft)}} = \text{lift from wing} / \text{drag from wing} + \text{other drag} \quad (2.5)$$

The net aerodynamic forces act through a point which is called the center of pressure (CP). The center of pressure coefficient is the ratio of the distance of the CP from the leading edge to the chord length, which is given in percentage of the chord length behind the leading edge. The location of CP will change when the pressure around the body changes. It moves forward if the angle of attack increase and backward if the angle of attack decrease [Kroes and Rardon, 1993]. CP is important in the consideration of trimming the aircraft and also the stability. However CP difficult to obtain. Normally, the aerodynamic center (AC) is used by researchers to determine the concentrated aerodynamic

forces location. The location of AC is $\frac{1}{4}$ chord behind the leading edge and it does not move with the angle of attack.

2.1.2 Reynolds Number

In 1883, Osborne Reynolds introduced a dimensionless parameter which gave a quantitative indication of the laminar to turbulent flow. For flow of water in the pipe, the flow is in laminar below Reynolds number 2100. Transition region is in between Reynolds number 2100 to 4000 and turbulent flow has a Reynolds number greater than 40000 [Talay, 1975]. Reynolds number depends on the chord length, velocity and properties of fluid at different altitudes. High Reynolds number is achieved with large chord length, high velocity and low kinematics viscosity. Most of the airfoils operate at several million Reynolds number.

The Reynolds number is expressed as:

$$Re = \frac{\rho V X}{\mu} \quad (2.6)$$

where:

ρ = density of fluid, kg/m^3

V = mean velocity of fluid, m/s

X = characteristics length, m

μ = coefficient of viscosity, kg/m.s

Reynolds number is usually used in an aircraft design to take into account the scale effect and as an index to predict various types of flows.

2.1.3 Airflow around the airfoil

Figure 2.2 shows the streamlines around a two dimensional airfoil. At a small angle of attack, fluid particles will follow the streamline. The streamline slow down at the front of the leading edge. The point where the particles are slowing down and divided into two parts of surfaces is called stagnation point. The division of the streamline causes increase in velocity at the upper surface while at the lower surface, the velocity will decrease [Barnard and Philpott, 1995].

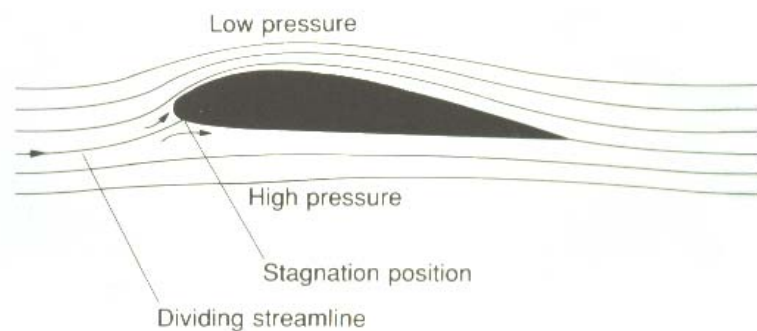


Figure 2.2: Streamlines around 2D airfoil [Barnard and Philpott, 1995]

A three dimensional view is shown in Figure 2.3. The flow is represented by the stream surface. It is observed that the dividing stream surface meets the wing section along a line just under the leading edge. The locus of stagnation position is called stagnation line.

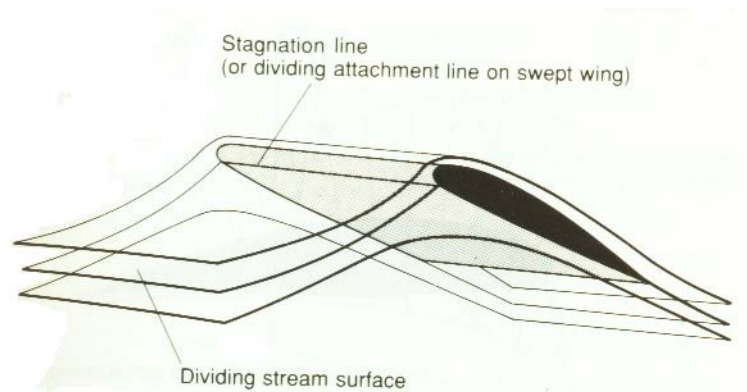


Figure 2.3: Stream surface [Barnard and Philpott, 1995]

There are two types of flow that exists in the viscous flow, laminar and turbulent flows. Anderson Jr. [1989] defines laminar flow as a flow where the streamlines are smooth and regular and a fluid element moves smoothly along the stream. Whereas, the turbulent flow is the flow where the streamline break up and a fluid element moves in a random, irregular and tortuous fashion. The presence of the friction in a flow caused a shear stress, τ_w which has a tangential direction to the surface which will give a drag force is called skin friction drag. The friction also causes a flow separation. It is due to the pressure on the rearward surface less than the pressure on the forward surface. This pressure difference causes what is called pressure drag due to separation.

Figure 2.4 shows the boundary layer separation. At the leading edge of the airfoil, the pressure is high. As the flow accelerates to the upper surface, the pressure is decreased to a minimum value, which is below the static pressure. As the flow is near the trailing edge, the pressure gets gradually increased. This

region of increasing pressure is called as a region of adverse pressure gradient [Anderson JR, 1989]; the pressure increases until it returns to a value close to the original free-stream pressure. It means that the air has to travel from the low to high pressure by slowing down and giving up some of the extra kinetic energy. Close to the surface inside the boundary layer, some of the available energy is dissipated in friction, and the air no longer return to its original free stream velocity.

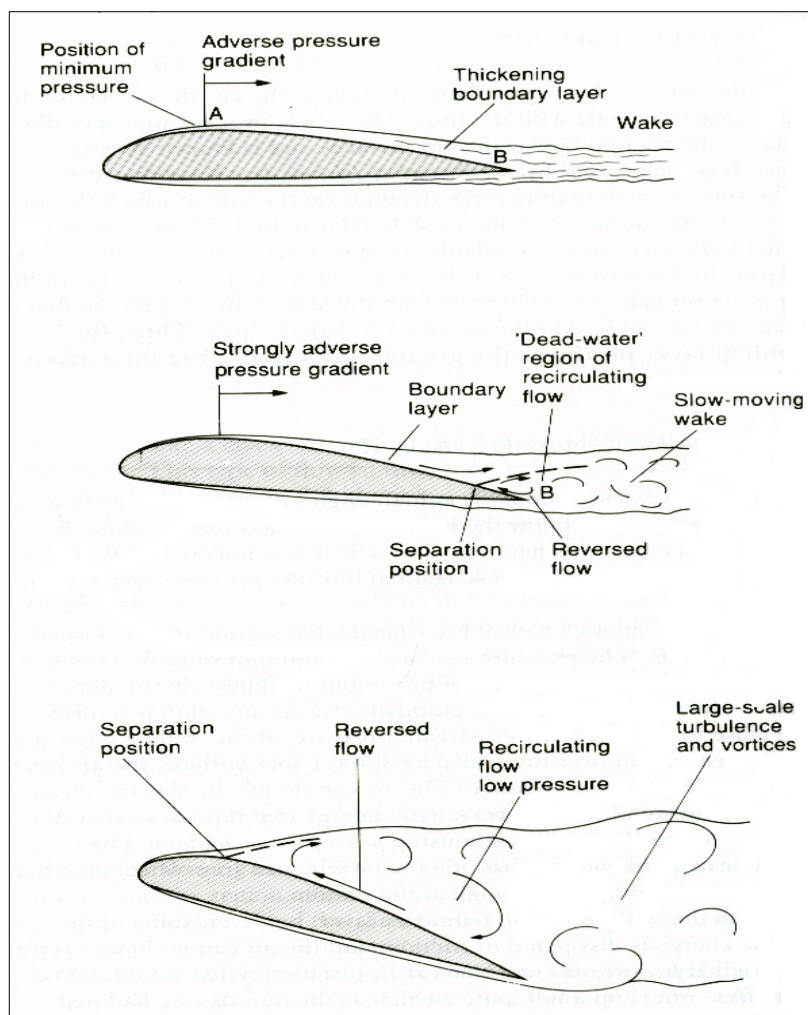


Figure 2.4: Boundary layer separation [Barnard and Philpott, 1995]

As the angle of attack is increased, at the leading edge, the pressure drops to a value far below the free stream static pressure. As the flow moves near the trailing edge, the rate of increase in pressure is rapid. The mixing process is too slow to keep the lower part of the layer moving and dead water region starts to form. The boundary layer stops following the mainstream and the flow is said to be separated. The flow field tends to separate from the surface and cause stalling [Barnard and Philpott, 1995].

2.1.4 Effect of vortices

When considering the three-dimensional flows around the airfoil, the effect of vortices has to be considered. The investigation of the vortices effect on the aircraft is important. Flows with minor disturbance are most desirable and it is a challenge subject for the researchers to study and obtain the solution. In the aircraft, the separation of flow and vortices are the most critical conditions which gives a deteriorating performance in an aircraft. Most of the conventional aircraft flight has turbulent flow. The turbulent flow contributes to increase in the drag coefficient. The researchers and scientists carry out lot of research to overcome this situation and try to improve.

For the three dimensional wing, the wing is exposed to the wind and the span wise flow occurs. The higher pressure at the lower surface spills out toward the wing tip to the upper wing. The pressure at the upper surface has a tendency to equalize the pressure. This causes the lift force per unit span to decrease near the wing tip. The spanwise pressure variation exists and as a result the incoming flow is inward towards the root at the upper surface and

outward at the lower surface. The flow from upper and lower surfaces joins at the trailing edge. The differences in spanwise velocity component will cause air to roll up and result in vortices as shown in Figure 2.5.

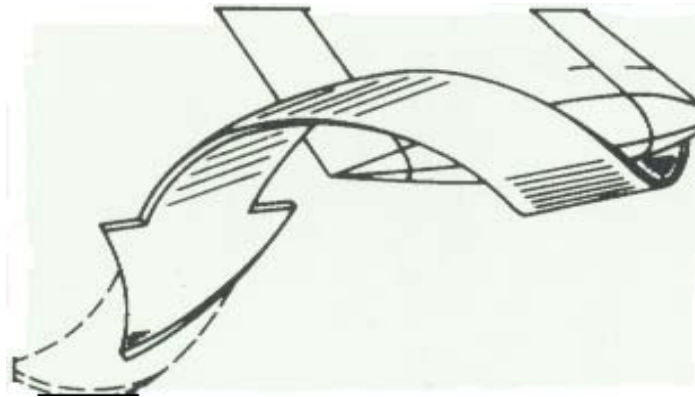


Figure 2.5: Formation of tip vortex [Bertin and Smith, 1998]

A short distance downstream, the vortices roll up and combine into two distinct cylindrical vortices [Bertin and Smith, 1998]. This situation is shown in Figure 2.6.

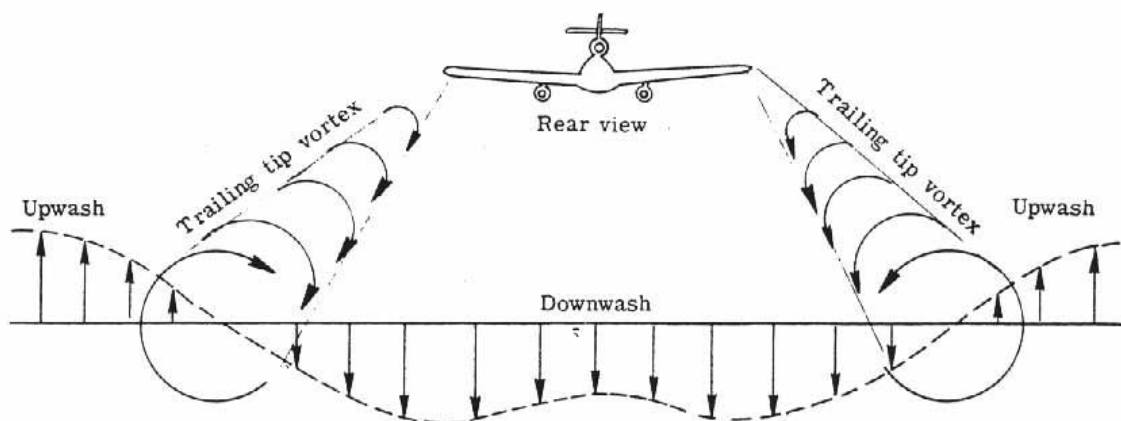


Figure 2.6: Vortex flow effect [Talay, 1975]

2.2 REMOTELY PILOTED VEHICLE

2.2.1 History of flight:

The history of flight began when human keep questioning the ability of the bird to fly. Pre historic man copies the action from the bird. In the year around 1500, Leonardo da Vinci found that the movement of the wing will produce a resulting force. From that, he invented Ornithopters, the machines that were intended to copy the bird's wing-the muscle power being supplied by man. This attempt failed. Instead it was based on the concept lighter-than -air, Mongolfier brothers from France, constructed a hot air balloon in 1783 and they achieved a height of 6000 ft in a balloon with a diameter of more than 100 ft. After that, Sir George Cayley (1773-1857), known as a 'Father of Modern Aerodynamic' built a glider with a wing and tail. He suggested on idea to have a fixed wing for generating lift and a combined horizontal and vertical tail for stability. He discovered that the basic force acting on a wing and the increasing angle of attack of wing will produce higher lift. At the end of 19th century, a German named Otto Liliental first successfully flew a glider of his own design. Later, Orville and Wilbur Wright from Ohio built an improve glider based on Otto Liliental's experimental result. In 1896, Dr Samuel Pierpont Langley designed small steam-power aircrafts and on December, 1903, the Wright brothers achieved success in a gasoline engine-powered machine named Wright Flyer 1. Starting from this, the evolution of aviation and aerodynamic has developed. Wright brothers built aircrafts based on their studies which are Flyer 2, Flyer 3 and Wright Type A in 1908 [Talay,1975].

2.2.2 History and development of RPV and UAV

The concept of pilotless vehicle is not new. It has been developed before the World War I. In World War II, the Germans developed the V-1 “Buzzbomb” rocket, with the concept of pilotless vehicle. It is a simple unmanned aircraft with a wingspan of about 19 ft and overall length of 26 ft. Besides that, they were also produced by the Allied Forces and used for photo reconnaissance task. After that, the UAVs were seen as a potential reconnaissance platform which was done in Vietnam War. The modified Teledyne-Ryan AQM-34 Firebee jet powered target was used for damage-assessment mission [Gerken, 1991].

The RPV and UAVs are mostly used for the military purposes. Recently, the UAVs have been used in all major conflicts including those in the Persian Gulf, Kosovo, Afghanistan and Iraq. The success of UAV in the Persian Gulf indicates usefulness of UAV in obtaining timely intelligence during modern military conflicts. The Pioneer, remotely piloted vehicle, has served in fleet and ground operation since 1987. Pioneer air vehicle logged 1011 hours during 307 flights in Operation Desert Storm [Howard et.al, 1996]. Similarly, the endurance of the UAV Predator, equipped by the ordnance, was credited as the first UAV with the precision strike capability, when it stalked Taliban and Al-Qaeda leaders in Afghanistan War, by striking these targets with Hellfire missiles [Ciufo, 2003]. In Iraq war, eleven types of UAV [www.auvsi.org] were used in the war for the field duties. In the war, most of the UAVs are deployed for surveillance, reconnaissance, and observation and targeting. Desert Hawk,

Dragon Eye, Global Hawk, Pioneer, Pointer and Predator are the common UAVs that have been deployed for these tasks.

In Malaysia, the first unmanned aerial vehicle was based on the Eagle 150 ARV aircraft. The system has a ground control unit and it can also be handled by remote control. The navigation was made through a highly sensitive video camera. So far, Malaysian Government has spent about RM47 million on the UAV and has been fully operational in year 2002. The UAVs have to fulfill the task of monitoring the country's border line, surveillance, spying operations and as a jammers in electronics warfare. The UAV can fly for about 10 hours, with the effective range of 220km. It can carry payload of about 60kg and has a radar system for multiple task of surveillance. In the research field, the Department of Aerospace Engineering, Universiti Putra Malaysia is intensively involved in UAV development. The UAV is expected to be completed in the year 2006 with the mission tasks of agricultural, surveillance and weather sampling. It is designed to be fully controlled by the ground station unit with the absence of pilot. The UAV is expected to fly for about 24 hours and at the highest service ceiling of about 500 ft [Jamlus, 2004].

The RPVs are capable to carry camera, sensors, missiles, acoustic instrument, air particle sampler and chemical agent detector depending on the mission. Nowadays, many aircrafts, which are based on the unmanned aerial vehicle system, exists in the market. Micro Aerial Vehicle (MAV) is the smallest aircraft. Due to its small size, it has an advantage of ability to fly unnoticed in battlefield. Tactical UAV is an aircraft, which is designed to operate at radius of

100 to 500 km with about 2 to 7 hours endurance while Endurance UAV is designed to operate at a high altitude with endurance exceeding 24 hours.

The RPV and UAV have designs of varying dimensions, weight, endurance and speed for vision objective requirements. Usually, for the long endurance task, the UAV is bigger, heavier and faster. Data of UAV in the market today with its specification is presented in Table 2.1 [www.auvsi.org]. Commonly, the materials that are used to develop the UAV must be damage resistant and designed for limited field repairs. Examples of UAV materials are fiberglass composites and aluminum. The power plant, which power the RPV and UAV are usually the electronic propulsion system, turbofan engine, piston engine or electric motor powered by batteries. The launch and recovery of the automated aircraft are done in many ways. For example: hand launched, autopilot commanded, wheeled, rocket assisted take off, track mounted hydraulic catapult, parachute and airbag.

One of the areas of interest is the aerodynamic performance and design of the RPV. This is because of the various shapes of wing and fuselage design, launch and recovery at low Reynolds number flying condition. Figure 2.7 shows in different configurations of RPV and UAV. Due to limited information about the performance of the various shapes of the RPV and UAV designs, research centers and universities are doing extensive research on RPV development and performance.

Table 2.1 : The data of UAV [www.auvsi.org]

| Name of UAV and RPV | Dimension | | | Weight | | | Performance | | | | |
|------------------------|----------------|----------|--------|--------|-------|----------|-------------|--------------|-----------|-----------|---------------|
| | Overall length | Wingspan | Height | MTOW | Empty | Payload | Max.speed | Cruise speed | Endurance | Max.Range | Max. Altitude |
| | (m) | (m) | (m) | (kg) | (kg) | (kg) | (km/h) | (km/h) | (hr) | (km) | (m) |
| Brumby | 1.97 | 2.82 | n.a | 35 | 19 | 14 | 185 | 72 | 1 | | |
| Fox AT1 | 2.75 | 3.60 | n.a. | 85 | 55 | 20 | n.a | 150 | 3 to 4 | 166 | 4000 |
| Fox AT2 | 2.75 | 3.60 | n.a | 125 | 65 | 25 | n.a | 150 | 3 to 5 | 166 | 4000 |
| Half-Scale UAV Trainer | 1.9 | 2.5 | 0.5 | 18.1 | 12.7 | 4.5 | 148 | n.a | 1 | n.a | n.a |
| Kestrel 11 | 4 | 5 | n.a | 120 | n.a | 25 to 30 | 185 | n.a | 5 | n.a | 2500 |
| Micro V | 2.85 | 3.60 | n.a | 45 | 27 | 8 | 185 | 118 | 5 | 50 | 4575 |
| Mirach 26 | 3.85 | 4.73 | 1.27 | 200 | 186 | 50 | 220 | 145 | 6 | 100 | 3500 |
| Pioneer (RQ-2A) | 4.26 | 5.11 | 1.2 | 203 | n.a | 45 | 176 | n.a | 6 | 185 | 3660 |
| Shadow 200-T | 3.10 | 3.89 | 0.86 | 127.3 | 83.2 | 28.2 | 194 | 135 | 4 | 50 to 200 | 4500 |
| Shadow 200 | 3.40 | 3.9 | 0.89 | 148.6 | 91 | 25.3 | | 155 | 5 to 6 | 200 | 4573 |
| Sojka 111 | 3.83 | 4.12 | 1.07 | 145 | 125 | 20 | 180 | n.a | 3 | 100 | 3000 |
| Annasnas Mk I | 2.8 | 3.80 | 1.3 | 125 | 43 | 25 | 130 | n.a | 14 | n.a | 5000 |
| Shadow 400 | 3.82 | 5.1 | | 201 | 147 | 30 | | 139 | 5 | | 3660 |
| Shadow 600 | 4.8 | 6.8 | | 265 | | 41 | | 139 | 12 to 14 | | 4877 |
| Desert hawk | 0.732 | 1,158 | | 1,888 | | 0.373 | | | 1.5 | | |

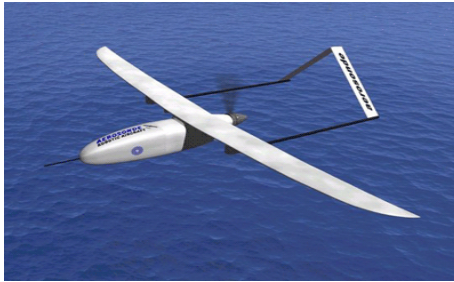


Figure 2.7: The RPV and UAV with different configuration [www.auvsi.org]